DSMC simulation of rarefied gas flows under cooling conditions using a new iterative wall heat flux specifying technique

H. Akhlaghi, E. Roohi, and R. S. Myong

Citation: AIP Conf. Proc. 1501, 687 (2012); doi: 10.1063/1.4769609
View online: http://dx.doi.org/10.1063/1.4769609
View Table of Contents: http://proceedings.aip.org/dbt/dbt.jsp?KEY=APCPCS&Volume=1501&Issue=1
Published by the American Institute of Physics.

DSMC Simulation of Rarefied Gas Flows under Cooling Conditions Using a New Iterative Wall Heat Flux Specifying Technique

H. Akhlaghi[a], E. Roohi[a], and R. S. Myong[b]

[a]*Department of Mechanical Engineering, Ferdowsi University of Mashhad, P.O. Box 91775-1111, Mashhad, Iran*
hassan.akhlaghi@gmail.com
e.roohi@um.ac.ir

[b]*Department of Aerospace and System Engineering, Research Center for Aircraft Parts Technology, Gyeongsang National University, Jinju, Gyeongnam 660-701, South Korea*
myong@gnu.ac.kr

Abstract. Micro/nano geometries with specified wall heat flux are widely encountered in electronic cooling and micro-/nano-fluidic sensors. We introduce a new technique to impose the desired (positive/negative) wall heat flux boundary condition in the DSMC simulations. This technique is based on an iterative progress on the wall temperature magnitude. It is found that the proposed iterative technique has a good numerical performance and could implement both positive and negative values of wall heat flux rates accurately. Using present technique, rarefied gas flow through micro-/nanochannels under specified wall heat flux conditions is simulated and unique behaviors are observed in case of channels with cooling walls. For example, contrary to the heating process, it is observed that cooling of micro/nanochannel walls would result in small variations in the density field. Upstream thermal creep effects in the cooling process decrease the velocity slip despite of the Knudsen number increase along the channel. Similarly, cooling process decreases the curvature of the pressure distribution below the linear incompressible distribution. Our results indicate that flow cooling increases the mass flow rate through the channel, and vice versa.

Keywords: DSMC, Wall Heat Flux Specified Boundary Condition, Iterative Technique, Cooling/Heating, Thermal Creep.

PACS: 47.61.−k, 47.45.−n, 05.70.−a, 02.70.−c

INTRODUCTION

Improvements in performance and shrinkage of device sizes in micro/nano electronics have been major driving forces for scientific and economic progress over the last years. There have been significant developments in micro/nano-electro-mechanical-systems (MEMS/NEMS) for measurement and manipulation at molecular and atomic levels. Consequently, a true understanding of the thermal behavior of rarefied micro/nano gas flows is crucial in design, fabrication, and operation of MEMS/NEMS [1-2]. Once the gas flow rarefies, the Knudsen number, defined as the ratio of gas mean free path to the characteristic length of the geometry, $Kn=\lambda/h$, increases and the flow analysis must be performed using accurate approaches based on the solution of the Boltzmann equation [3].

Despite the considerable efforts to derive higher order equations, discrete molecular modeling of direct simulation Monte Carlo (DSMC) is the key tool to model flow field in all degrees of rarefaction [4]. In DSMC, the gas is modeled as a collection of moving particles which interact through collisions. DSMC is known as one of the most successful particle simulation methods in analyzing the rarefied gaseous flows. Specified wall temperature (SWT) boundary treatment has been widely used to model the gas-surface interaction in DSMC. In addition to the SWT boundary treatment, there is serious demand in imposing the specified wall heat flux (SWH) boundary condition in many MEMS/NEMS applications, especially in electronic cooling. Typically, power-dissipating semiconductor devices in electronics MEMS/NEMS could be treated as heat generation sources embedded on flat surfaces [5-6]. Additionally, Modern electronic cooling requires dissipation of great amount of heat from tiny regions. In such applications, specified heat flux walls are more common than those with specified temperature. The previous works on wall heat flux implementation have mainly focused on negative wall heat flux values, i.e., heating application [7-9]. However, there is wide range of applicability of cooling process in electronic industry. Introducing

28th International Symposium on Rarefied Gas Dynamics 2012
AIP Conf. Proc. 1501, 687-694 (2012); doi: 10.1063/1.4769609

a simple algorithm motivated the authors to develop a general wall heat flux implementation method suitable for both heating/cooling applications. The rest of this paper organized as follows. We study both of negative and positive heat flux values and compare hydrodynamics and thermal behavior of micro/nano channel under different heat flux conditions.

DSMC MODELING AND GAS-SURFACE INTERACTION

DSMC is a numerical tool to solve the Boltzmann equation based on the direct statistical simulation of the molecular processes described by the kinetic theory [4]. The primary principle of DSMC is decoupling of the motion and collision for all simulated particles. DSMC is considered as a particle method in which one particle represents a large bulk of real gas molecules. When a particle collides to a surface, the energy is transferred in the form of heat and stress. This leads to two main types of accommodation coefficients known as thermal and transverse momentum coefficients. The thermal accommodation coefficient (α_c) represents the fraction of heat transferred between the surface and the particle and is calculated from [4]

$$\alpha_c = \left(E^i - E^r\right) \Big/ \left(E^i - E^w\right). \tag{1}$$

E^w is the reflected energy flux if the molecular reflective characteristic temperature be equal to the wall temperature $T_r=T_w$. Using the definition of thermal accommodation coefficient, we can ratify specular and diffusive walls. For specular wall, the molecular reflective characteristic temperature is equal to that of the incident molecule, $T_r=T_i$. In diffusive wall case, the molecular reflective characteristic temperature is equal to the wall temperature, $T_r=T_w$. According to these expressions, there is no energy transfer between wall and molecule for the specular wall, i.e., $\alpha_c=0$, and there is a complete thermal accommodation for diffusive wall, $\alpha_c=1$. In the DSMC method, the wall heat flux rate is defined as the difference between the incident and reflected energy fluxes per unit time and per unit area of the wall. The definition of wall heat flux rate for a cell surface is given by

$$q_w = \frac{\sum \varepsilon^i - \sum \varepsilon^r}{\Delta t.S}. \tag{2}$$

The incident and reflected energy fluxes are obtained by summing up the incident and reflected energy of the molecules colliding to the surface.

ITERATIVE TECHNIQUE

We introduce a new technique named as "Iterative Technique" to implement both negative and positive wall heat flux rate values. The foundation of the iterative technique is based on the correction of the wall temperature during the DSMC simulation. We calculate wall temperature from the following relation

$$\begin{aligned} T_w^{new}(x) &= T_w^{old}(x) + \Delta T_w(x) \\ \frac{\Delta T_w(x)}{T_w(x)} &\propto \frac{q_w(x) - q_{des}(x)}{\left|q_{des}(x)\right|} \\ T_w^{new}(x) &= T_w^{old}(x)\left(1 + \mathrm{RF}\frac{q_w(x) - q_{des}(x)}{\left|q_{des}(x)\right| + \varepsilon_0}\right). \end{aligned} \tag{3}$$

Equation (3) is a local relation which is applied to every wall boundary cells in the domain. We should define wall temperature correction values $\Delta T_w(x)$ such that the iterative algorithm converges and the final wall temperature distribution becomes physical. According to Eq. (2), positive values of wall heat flux means that heat transfer from flow to the wall, i.e., cooling, and negative value showed that heat transfers from the wall to the flow, i.e., heating. Since total energy of reflected molecule is proportional to the wall temperature, higher wall temperature

values result in more negative wall heat flux rates. Therefore, from the stability point of view, $\Delta T_w(x)$ must satisfy the following conditions

$$\begin{aligned} &\Delta T_w(x) > 0 \;\; if \;\; q_w(x) > q_{des}(x) \\ &\Delta T_w(x) < 0 \;\; if \;\; q_w(x) < q_{des}(x). \end{aligned} \tag{4}$$

According to Eq. (4), wall temperature correction for each boundary cell should be adjusted considering local heat flux rate of that cell. To apply this criterion, we introduce a non-dimensional proportionality based on conditions given by Eq. (4)

$$\frac{\Delta T_w(x)}{T_w(x)} \propto \frac{q_w(x) - q_{des}(x)}{\left|q_{des}(x)\right|}. \tag{5}$$

The stability criteria given by Eq. (4) are well considered in the suggested proportionality, i.e., Eq. (5), for both positive and negative values of desired wall heat flux rates. With the substitution of Eq. (5) in Eq. (3), we have

$$T_w^{new}(x) = T_w^{old}(x)\left(1 + \mathrm{RF}\frac{q_w(x) - q_{des}(x)}{\left|q_{des}(x)\right| + \varepsilon_0}\right) \tag{6}$$

where *RF* is a relaxation factor to control the convergence progress and avoid solution divergence. RF must be adjusted in a manner which ensures the best convergence behavior. Based on our numerical experiences, RF should be considered no greater than 0.03. The RF values greater than 0.03 may lead to divergence. However, it is observed in several simulation cases that RF could be considered up to 0.1 without divergence penalty. ε_0 is a non-zero and positive value which is negligible with respect to the incident energy fluxes. It is defined for adiabatic wall cases, i.e., $q_{des} = 0$. Eq. (6) is called as "Iterative Equation" which implements a desired heat flux rate distribution by correcting the wall temperature. There must be an initial wall temperature distribution to start the iterative technique. We could use any desired initial wall temperature distribution, i.e., uniform distribution. Figure 1 shows the schematic algorithm of the iterative technique. During one wall sampling period Δt, a specified wall temperature or classical DSMC simulation is performed and incident and reflected energy fluxes for all wall cells are sampled. At the end of sampling period Δt, local wall temperature values $T_w(x)$ are obtained by Eq. (6) and an updated wall temperature distribution is used for the DSMC simulation on the next sampling period. It should be noted that there is no additional complexity in the use of our iterative technique for flow with multiple species.

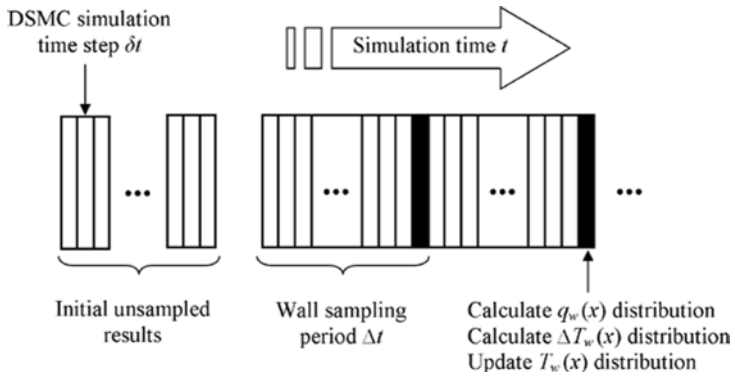

FIGURE 1. Schematics of the iterative technique algorithm.

HYDRODYNAMIC AND THERMAL BEHAVIOR OF THE FLOW FIELD UNDER POSITIVE WALL HEAT FLUX

In this section, we study the effects of different wall heat flux rates on the hydrodynamic and thermal behavior of the flow field. Figure 2 shows the convergence behavior of wall temperature for different values of relaxation factor (RF=0.01, 0.03, and 0.06) and simulation time. The higher values of RF lead to the faster convergence. The final wall temperature distributions for RF values of 0.01, 0.03, and 0.06 are obtained at t=8×10^5 NPR, t=4×10^5 NPR, and t=2×10^5 NPR, respectively. Wall temperature decreases along the channel. From the physical point of view, as the flow moves down along the channel, bulk temperature drops. To have a constant heat flux along the wall, wall temperature also decreases.

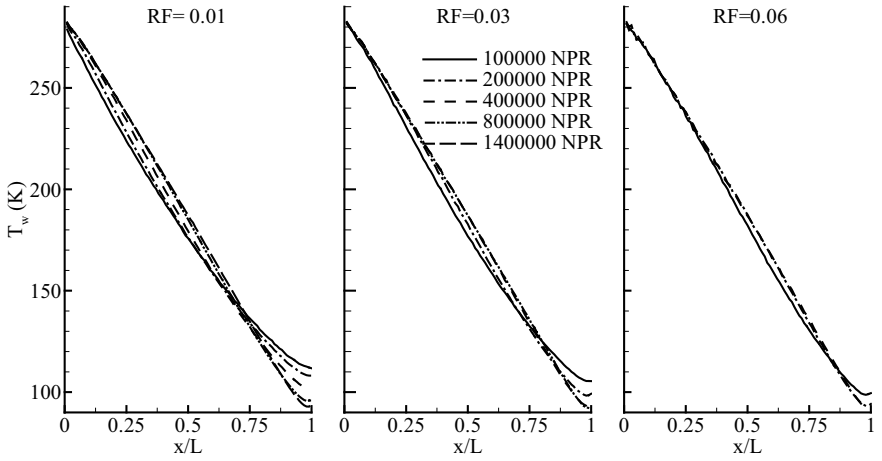

FIGURE 2. Effect of relaxation factor on the convergence of computed wall temperature, q_{des}= 4×10^6.

Figure 3 shows the temperature fields for different wall heat flux rate magnitudes. Temperature fields for negative (q_{des}= -4×10^6 W/m), zero, and positive (q_{des}= 4×10^6 W/m) wall heat flux rates are shown. According to the figure, temperature increases along the channel for negative heat flux and decreases for positive wall heat flux rate condition. It is because of energy transfer from the wall to the flow or via versa. There is no gas-surface energy transfer in adiabatic wall case. However, temperature decreases because of the gas flow acceleration along the channel.

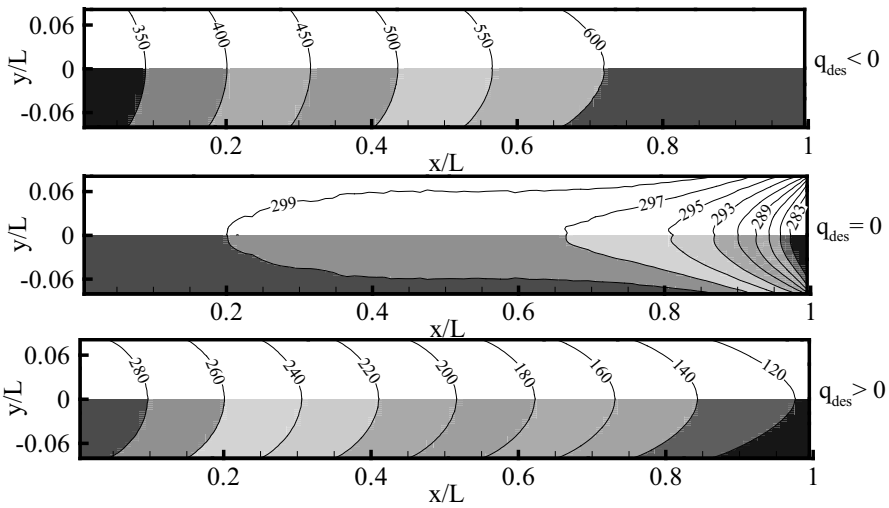

FIGURE 3. Temperature fields for different values of wall heat flux rate.

The effects of gas-surface energy transfer on the rarefaction of the flow field are shown in Fig. 4. This figure denotes distribution of centerline Knudsen number for negative, zero, and positive q_{des} values. For all cases, the results show that the flow rarefies along the channel due to flow acceleration. The most and least rarefied flows are attained for negative and positive values of q_{des}, respectively. As energy transfers from the wall to the flow, density decreases and flow rarefies more since the pressure ratio is kept constant along the channel. Consequently, rarefaction increases with heat addition to the flow and decreases with the heat subtraction by the walls. Figure 4 shows that the rate of Knudsen increasing is faster for negative values of q_{des}. Interestingly, we observe that variation of Knudsen number for positive heat flux is quite small. It means that increase in rarefaction due to flow acceleration is almost balanced with the decrease supposed by the heat transfer to walls. This observation suggests cooling process as a useful strategy to minimize variation of the density field in MEMS/NEMS.

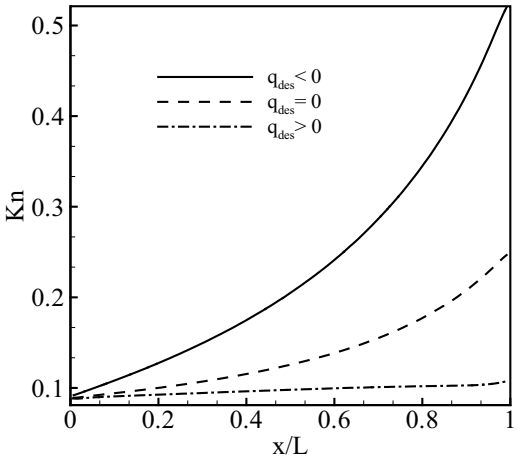

FIGURE 4. Knudsen number distributions along the channel for different values of wall heat flux rate.

Figure 5 shows the effect of various values of q_{des} on the pressure distribution and pressure deviation from the linear distribution along the channel. Fig 5(a) plots pressure distributions for negative, zero, and positive values of q_{des}. According to this figure, pressure increases for more negative values of q_{des}. The effect of rarefaction is to reduce the curvature in the pressure distribution while compressibility increase curvature and lead to a more nonlinear pressure distribution along the channel [10-11, 14]. According to Fig. 5(a), the effect of compressibility on the pressure distribution is dominant compared to that of rarefaction for adiabatic and negative q_{des}. However, heat addition to the flow increases both rarefaction and compressibility effects, as shown in Figs. 4 and 5. Interestingly, curvature is positive for positive q_{des}. In other words, pressure distribution is below linear incompressible one if we effectively cool down the flow field; see Fig. 5(b). This behavior may be attributed to the thermal creep effect. For $q_{dse}>0$ case, wall temperature falls from 280K to 90K. As is known, thermal creep leads to an induced flow and pressure gradient from the cold region to the hot one [10]. This negative pressure gradient counteracts positive pressure distribution along the channel. This effect is negligible for the zero q_{des} case because there is small variations in the wall temperature for this condition, namely from 300K to 307K along the channel. Thermal creep effect is concurrent with the compressibility one and both effects increase pressure curvature along the channel.

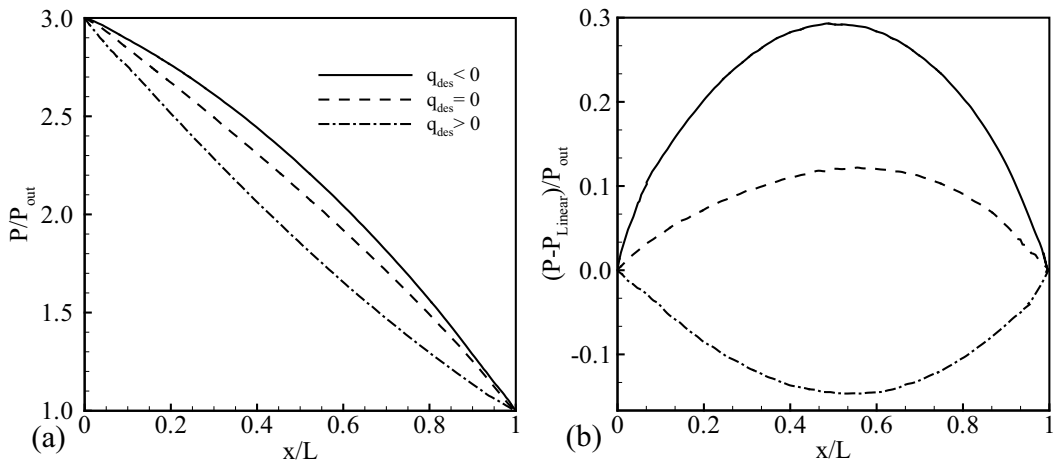

FIGURE 5. (a) Pressure distributions, and (b) pressure deviation from the linear distribution, along the channel for different values of wall heat flux rate.

Figure 6 shows the effect of different q_{des} values on the velocity profiles at the initial, middle, and terminal sections of the channel. Left, center, and right graphs plot velocity profiles for the negative, zero, and positive values of q_{des}, respectively. The velocity profile is non-dimensionalized to its magnitude at the centerline, U_c. We observe minimum and maximum variations in the velocity slip for the $q_{des}>0$ and $q_{des}<0$ conditions, respectively. This behavior is attributed to the Knudsen number variation along the channel, i.e., largest variation is observed for negative heat flux case and smallest variation is observed for positive heat flux case. It is expected that velocity slip increases along the channel as the flow rarefaction increases [15]. However, positive heat flux ($q_{des}>0$) case shows different behavior and velocity slip slightly decreases despite of increase in the gas flow rarefaction. However, velocity slip variations are very small in this case, see Fig. 6. Again, we could attribute this behavior to the thermal creep effects. Thermal creep effects produce an additional slip velocity which is directed to the cold region [10]. This effect is concurrent in the $q_{des}<0$ case and increases the velocity slip along the channel, but it leads to a negative velocity slip in $q_{des}>0$ case. According to Fig. 6, it is well seen that thermal creep effect is dominant compared to the rarefaction effect for $q_{des}>0$ case. In case of zero q_{eds}, wall temperature variation is small and thermal creep effect is negligible. Consequently, velocity slip increases along the channel as flow rarefies more.

The effect of the heating and cooling processes on the mass flow rate of the channel is investigated in Fig. 7. The results are compared with those of Wang *et al*. [8], which correspond to the flow heating simulation. By comparison, it is well seen that there is a good agreement between current results with those of Ref. [8]. According to this figure, the flow heating by the walls decreases mass flow rate through the channel, and vice versa. The rate of mass flow rate increase is faster for more positive values of q_{des}. The increase in mass flow rate for this condition could be attributed to smaller decrease in the density field along the channel for cooling conditions, see Fig. 4. According to this observation, we could use normal heat flux parameter as a suitable tool to control and adjust desired mass flow rate in micro/nano devices.

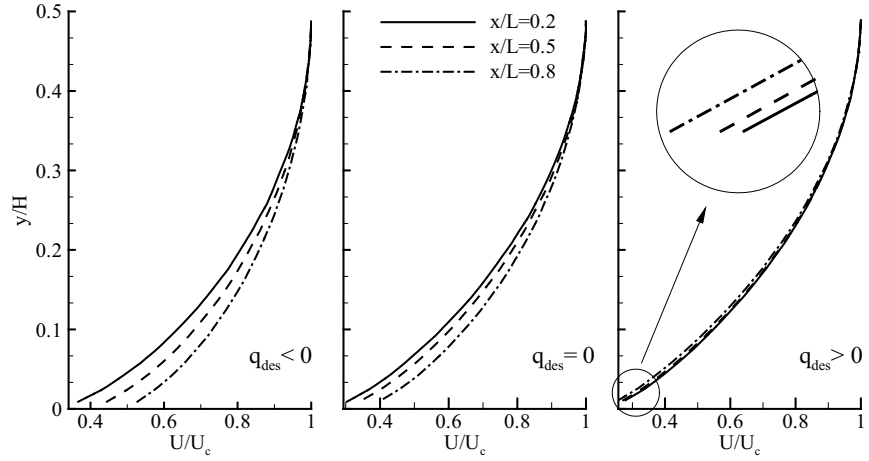

FIGURE 6. Velocity profiles along the channel wall for different values of wall heat flux rate.

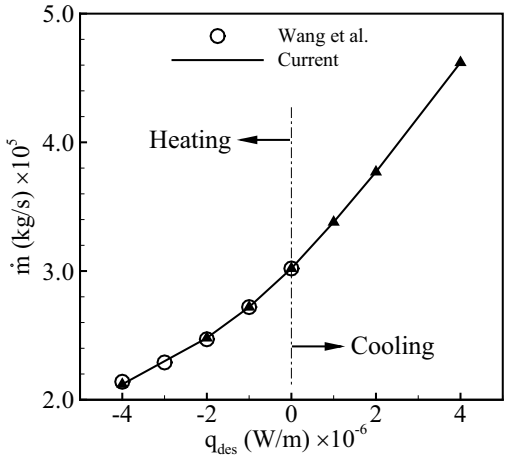

FIGURE 7. Dependence of the mass flow rate on the wall heat flux values and comparison of the current results with those of Wang *et al*. [8].

CONCLUSIONS

We introduced a new technique to implement desired wall heat flux rate in the DSMC method for MEMS/NEMS applications. This technique was based on an iterative progress on the wall temperature magnitude. It was found that the proposed iterative technique has a good numerical performance and could implement both positive and negative values of wall heat flux rates accurately. A relaxation factor (RF) was introduced to ensure the convergence of the iterative technique. It was shown that higher values of RF results in faster convergence. However, there are divergence risks if high values of RF are used. We extended our study and evaluated the effect of the number of simulator particles on the accuracy of the iterative technique. Our study showed that the effect of number of simulator particles is negligible on the achieved wall temperature distribution while it has considerable effect on the wall heat flux distribution. It is observed that cooling of micro/nano channel would result in small variations in the Knudsen number along the channel. If designers would like to increase the mass flow rate and prevent excessive rarefaction at the outlet of micro/nano devices, they should develop and utilize effective tools to cool down these devices. Similarly, our results detected that there is a positive curvature in pressure distribution for positive heat flux wall boundary condition. In other words, pressure distribution is well below the linear incompressible distribution for cooling condition. We observed that upstream thermal creep results in a small decrease in velocity slip magnitude along the channel in cooling condition. This behaviour is observed even though Knudsen number (rarefaction effects) increases as the flow approaches the outlet. We also simulated 2-D cavity flow under different

heat flux boundary conditions and studied hydrodynamics and thermal behaviours. It is observed that heating and cooling of the flow field is more effective at higher Knudsen number cases due to increasing non-equilibrium effects.

ACKNOWLEDGMENTS

The authors from Ferdowsi University would like to acknowledge the financial supports provided by the Faculty of Engineering, Ferdowsi University of Mashhad under Grant No. 18888/2. R.S.M. wishes to acknowledge the support from the National Research Foundation of Korea (grant no. NRF-2011-0031383) and partially by the Degree and Research Center for Aerospace Green Technology (DRC) funded by the Korea Research Council of Fundamental Science & Technology (KRCF).

REFERENCES

1. Z. M. Zhang, *Nano/Microscale Heat Transfer*, McGraw-Hill, New York, 2007.
2. C. M. Ho and Y. C. Tai, *Annu. Rev. Fluid Mech.* **30**, 579–612 (1998).
3. C. Cercignani, *The Boltzmann equation and its applications*, Springer, New York, 1987.
4. G. A. Bird, *Molecular Gas Dynamics and the Direct Simulation of Gas Flows*, Oxford. U.K.: Oxford Science, 1994.
5. F. P. Incropera, *J. Heat Transf.* **110**, 1097–1111 (1988).
6. S. Banerjee, A. Mukhopadhyay, S. Sen, and R. Ganguly, *Int. J. Therm. Sci.* **47**, 1516–1527 (2008).
7. Q. W. Wang, C. L. Zhao, M. Zeng, and N. Y. E. Wu, *Numer. Heat Tr. B* **53**, 150-173 (2008).
8. Q. W. Wang, C. L. Zhao, M. Zeng, and N. Y. E. Wu, *Numer. Heat Tr. B* **53**, 174-187 (2008).
9. Q. W. Wang, X. Yan, and Q. He, *Int. J. Numerical Methods in Engineering* **74**, 1109-1127 (2008).
10. G. Karniadakis, A. Beskok, and N. Aluru, *Microflows and Nanoflows,* Springer Science, 2005.
11. E. B. Arkilic, M. A. Schmidt, and K. S. Breuer, *J. Microelectromech. S.* **6**, 167–178 (1997).
12. W. Liou and Y. Fang, *Computer Modeling in Engineering & Science* **1**, 119-128 (2000).
13. M. Wang and Z. Li, *Int. J. Heat Fluid Fl.* **25**, 975-985 (2004).
14. M. Darbandi and E. Roohi, *Int. Commun. Heat Mass* **39**, 439-448 (2011).
15. R. S. Myong, *Phys. Fluids* **23**, 012002 (2011).